

parameters (including changes in the wavelength dependence) and pulsation activity in the supergiant with a period of 94^d.

We also need further study of the magnetic field: is there one present, how large is it, and what is its structure in the vicinity of the accretion disk? How much effect does it have on the wavelength dependence of the polarization?

- Aslanov, A. A., Kolosov, D. E., Dipunova, N. A., et al. (1989). *Catalog of Close Binary Stars in Late Stages of Evolution* [in Russian], Izv. MGU, Moscow, p. 82.
- Beskrovnaya, N. G. (1988). *Pis'ma Astron. Zh.* **14**, 737 [*Sov. Astron. Lett.* **14**, 314 (1988)].
- Bradt, H. V., Doxsey, R. E., and Jernigan, J. G. (1979). *X-ray Astronomy*, W. A. Baity and L. E. Peterson (eds.), Pergamon Press, p. 3.

- Brown, J. C., McLean, I. S., and Emslie, A. G. (1978). *Astron. Astrophys.* **68**, 415.
- Bugaenko, O. I. and Gural'chuk, A. L. (1985). *Photometry and Polarimetry of Celestial Objects* [in Russian], Naukova Dumka, Kiev, p. 160.
- Dolan, J. F. and Tapia, S. (1988). *Astron. Astrophys.* **202**, 124.
- Dupree, A. K., Gursky, H., Black, J. H., et al. (1980). *Astrophys. J.* **238**, 969.
- Gnedin, Yu. N. and Silant'ev, N. A. (1980). *Pis'ma Astron. Zh.* **6**, 344 [*Sov. Astron. Lett.* **6**, 190 (1980)].
- Karitskaya, E. A. and Bochkarev, N. G. (1983). *Astron. Zh.* **60**, 946 [*Sov. Astron.* **27**, 546 (1983)].
- Lovelace, R. V. E. (1976). *Nature* **262**, 649.

Translated by D. J. Mullan

A study of Cepheid period variability. Technique

L. N. Berdnikov

Saratov State University

(Submitted January 16, 1992)

Pis'ma Astron. Zh. **18**, 519–527 (June 1992)

An algorithm is described for computer implementation of the Hertzsprung method, the most accurate method of determining the times of brightness extrema of variable stars with stable light curves. A numerical experiment is performed, and a relationship obtained between the error σ in determining the times of Cepheid light maxima, the rms error in the observations σ_m , expressed in fractions of the amplitude, and the number of observations n : $\sigma = \sigma_m (0.453/\sqrt{n} + 2.51/n^2)$. Practical recombinations are made to account for the effects of noncoincident times of Cepheid maxima recorded in the Johnson *B* and *V* bands.

Introduction. The study of variable star period variability is based on analysis of *O* – *C* diagrams. The most accurate method of determining the *O* – *C* residuals (for stars with stable light curves) is the Hertzsprung method (Tsesevich, 1971). One of the advantages of this method is the ability to calculate the errors in determining the times of brightness extreme, but one of its drawbacks is the large number of calculations required, which probably is why the Hertzsprung method was not widely used in the days of manual calculations.

Widespread application of the Hertzsprung method became practical only with the advent of computers. In this work, several questions are examined pertaining to computer implementation of this method. For specific examples, we will use Cepheid light curves, although the Hertzsprung method is completely applicable to any variable star with constant light curve shape.

Computational method. In the Hertzsprung method, the mean light curve to be processed is superimposed by the least squares method on an actual (standard) curve constructed from the most accurate (for example, photoelectric) observations. The shift for which the observations coincide with the standard curve determines the phase of maximum light (which has the sense of an *O* – *C* residual, expressed in fractions of the period) which, when multiplied by the period, gives the *O* – *C* residual in days. Here, of course, the observations should first be transformed to the photometric system of the standard curve.

In the computer implementation of the Hertzsprung method, some difficulties are encountered when transforming the observations to the system of the standard curve. By using chords (Tsesevich, 1971), this transformation can be done for observations which fully span the light curve. However, the observations occasionally fall only on the rising or descending branch of the light curve, or are concentrated near maximum or minimum light. Increasing the number of points on the curve (as is possible when a large series of observations is processed piecemeal) does not always improve the situation, due to the sparsity of essentially all existing series of observations. This leads to a significant prolongation of the time interval, which can increase the scatter of points on the processed curve when the period is not accurately known (either poorly determined, or simply variable), or when the processed data include period change. Therefore, it is not always possible to construct a sufficient number of chords, and other methods of transformation, specific to each case, must be applied.

To alleviate these difficulties, we (Berdnikov, 1983) suggested implementing the Hertzsprung method somewhat differently from the classical approach: we proposed to approximate the actual observations, instead of the mean light curve, by the standard curve. For each observation we write an equation of condition of the form:

$$m_i = m_{av} + af(\psi_i, \psi), \quad (1)$$

where m_i is the observed magnitude, m_{av} is the average stellar magnitude, a is the half-amplitude of the oscillations, f is

TABLE I

n	σ_m	SZ Aql			U Aql			FN Aql		
		σ_m	Δ	σ	σ_m	Δ	σ	σ_m	Δ	σ
1	2	3	4	5	6	7	8	9	10	11
10	0.01	0.008	0.0000	0.0017	0.013	0.0002	0.0023	0.018	0.0005	0.0030
10	0.02	0.016	-0.0004	0.0031	0.027	-0.0008	0.0046	0.036	0.0005	0.0061
10	0.03	0.024	0.0001	0.0048	0.040	-0.0001	0.0076	0.054	0.0009	0.0094
10	0.04	0.032	-0.0005	0.0065	0.054	0.0004	0.0084	0.072	0.0010	0.0117
10	0.05	0.041	-0.0011	0.0079	0.067	0.0023	0.0107	0.089	0.0036	0.0144
10	0.07	0.057	0.0017	0.0109	0.094	0.0025	0.0172	0.125	0.0008	0.0220
10	0.10	0.081	-0.0014	0.0177	0.134	0.0065	0.0242	0.179	0.0009	0.0292
10	0.15	0.122	0.0036	0.0233	0.201	0.0086	0.0325	0.268	0.0097	0.0448
10	0.20	0.162	-0.0010	0.0358	0.268	-0.0073	0.0427	0.357	-0.0136	0.0550
10	0.25	0.203	0.0044	0.0410	0.335	0.0099	0.0533	0.447	-0.0142	0.0754
20	0.01	0.008	-0.0001	0.0009	0.013	0.0003	0.0014	0.018	-0.0001	0.0021
20	0.02	0.016	-0.0003	0.0016	0.027	-0.0002	0.0030	0.036	0.0003	0.0041
20	0.03	0.024	0.0003	0.0025	0.040	0.0004	0.0040	0.054	-0.0008	0.0060
20	0.04	0.032	0.0002	0.0034	0.054	0.0003	0.0058	0.072	0.0001	0.0081
20	0.05	0.041	0.0002	0.0042	0.067	0.0001	0.0068	0.089	-0.0003	0.0104
20	0.07	0.057	0.0002	0.0051	0.094	-0.0004	0.0096	0.125	-0.0020	0.0142
20	0.10	0.081	-0.0004	0.0081	0.134	0.0008	0.0141	0.179	0.0003	0.0206
20	0.15	0.122	0.0029	0.0117	0.201	0.0010	0.0206	0.268	-0.0100	0.0301
20	0.20	0.162	0.0018	0.0181	0.268	0.0008	0.0267	0.357	0.0036	0.0392
20	0.25	0.203	-0.0022	0.0207	0.335	0.0013	0.0338	0.447	-0.0069	0.0498
30	0.01	0.008	-0.0001	0.0006	0.013	0.0003	0.0011	0.018	-0.0002	0.0016
30	0.02	0.016	-0.0001	0.0013	0.027	-0.0001	0.0021	0.036	0.0000	0.0033
30	0.03	0.024	-0.0001	0.0019	0.040	0.0003	0.0033	0.054	-0.0005	0.0049
30	0.04	0.032	-0.0004	0.0024	0.054	-0.0004	0.0042	0.072	-0.0005	0.0065
30	0.05	0.041	0.0005	0.0033	0.067	0.0005	0.0053	0.089	-0.0001	0.0081
30	0.07	0.057	-0.0004	0.0043	0.094	0.0011	0.0075	0.125	-0.0018	0.0113
30	0.10	0.081	-0.0015	0.0066	0.134	0.0001	0.0103	0.179	-0.0018	0.0161
30	0.15	0.122	-0.0009	0.0092	0.201	-0.0024	0.0164	0.268	0.0069	0.0246
30	0.20	0.162	0.0023	0.0128	0.268	0.0014	0.0219	0.357	0.0009	0.0321
30	0.25	0.203	0.0006	0.0157	0.335	-0.0019	0.0284	0.447	-0.0032	0.0409
50	0.01	0.008	0.0001	0.0005	0.013	0.0001	0.0008	0.018	-0.0002	0.0012
50	0.02	0.016	0.0000	0.0009	0.027	0.0001	0.0017	0.036	0.0000	0.0025
50	0.03	0.024	-0.0001	0.0013	0.040	0.0002	0.0025	0.054	0.0002	0.0037
50	0.04	0.032	0.0002	0.0019	0.054	0.0001	0.0033	0.072	-0.0008	0.0049
50	0.05	0.042	-0.0001	0.0022	0.067	-0.0001	0.0041	0.089	0.0005	0.0061
50	0.07	0.057	-0.0003	0.0030	0.094	0.0003	0.0057	0.125	0.0008	0.0087
50	0.10	0.081	0.0003	0.0044	0.134	-0.0001	0.0082	0.179	-0.0001	0.0124
50	0.15	0.122	-0.0002	0.0070	0.201	0.0002	0.0126	0.268	0.0034	0.0190
50	0.20	0.162	-0.0005	0.0087	0.268	0.0002	0.0163	0.357	-0.0023	0.0242
50	0.25	0.203	0.0012	0.0112	0.335	0.0014	0.0204	0.447	0.0010	0.0307
100	0.01	0.008	0.0000	0.0003	0.013	0.0001	0.0006	0.018	-0.0001	0.0009
100	0.02	0.016	0.0001	0.0006	0.027	0.0000	0.0011	0.036	0.0005	0.0017
100	0.03	0.024	-0.0002	0.0009	0.040	0.0002	0.0017	0.054	0.0005	0.0026
100	0.04	0.032	-0.0001	0.0012	0.054	0.0004	0.0023	0.072	0.0008	0.0035
100	0.05	0.041	-0.0001	0.0015	0.067	0.0001	0.0029	0.089	0.0000	0.0043
100	0.07	0.057	0.0000	0.0021	0.094	-0.0004	0.0039	0.125	0.0000	0.0060
100	0.10	0.081	0.0005	0.0031	0.134	0.0000	0.0057	0.179	-0.0002	0.0087
100	0.15	0.122	0.0002	0.0046	0.201	0.0001	0.0086	0.268	-0.0016	0.0134
100	0.20	0.162	0.0002	0.0061	0.268	0.0008	0.0114	0.357	0.0028	0.0175
100	0.25	0.203	-0.0003	0.0075	0.335	0.0003	0.0143	0.447	-0.0012	0.0218

standard curve represented in tabular form and normalized to have amplitude in the interval $[1, -1]$, $\varphi_i(P)$ is the oscillation phase, which depends on period P , and ψ is the phase shift, which gives the phase of maximum light.

This approximation differs from a sine or cosine approximation only in that a standard curve, given in tabular form, replaces a trigonometric function in (1).

The system of nonlinear equations (1) is linearized and solved by the method of least squares for the corrections to any set of unknowns m_{av} , a , P , and ψ . As an initial approximation to m_{av} we take the arithmetic mean of all the processed stellar magnitudes; for we use the half-amplitude of the standard curve; for P we use the value given by the OKPZ (Organization of Variable Star Observers), and ψ is determined in the following manner: The sum of the squares of the deviations of the observations from the standard curve is calculated, then the standard curve is shifted in phase by 0.02 and the sum of the deviations squared is again calculated, then the standard curve is shifted another 0.02 and the sum of squares is again calculated, etc., until the total shift reaches 1. The shift corresponding to the minimum sum of squared deviations is then used as an initial approximation to ψ .

We note that m_{av} and a are obtained in the photometric system of the observer, and not of the standard curve, since the latter is given in dimensionless (normalized) form.

Besides the differences between this approach and the classical computational scheme (Tsesevich, 1971), there are also certain analogies. For example, m_{av} and a in Eq. (1) are responsible for the shift of the processed and standard curves along the stellar magnitude axis (i.e., the observations are transformed into the photometric system of the standard curve), and P and ψ are used to determine the phase of maximum light. If P is fixed, then for all intents and purposes, the proposed approach resembles the classical.

Numerical modeling. A computer program was written for the algorithm described above, and a numerical experiment was performed to test this program. Three typical Cepheid light curves were selected: a smooth curve with moderate amplitude and asymmetry; a curve with abrupt variations, large amplitude, and large asymmetry; and a small-amplitude, almost symmetric curve. As representatives of these we take the standard curves of U Aql, SZ Aql, and FN Aql, respectively. These standard curves were used to construct synthetic light curves. For each standard curve, shifted in phase by a

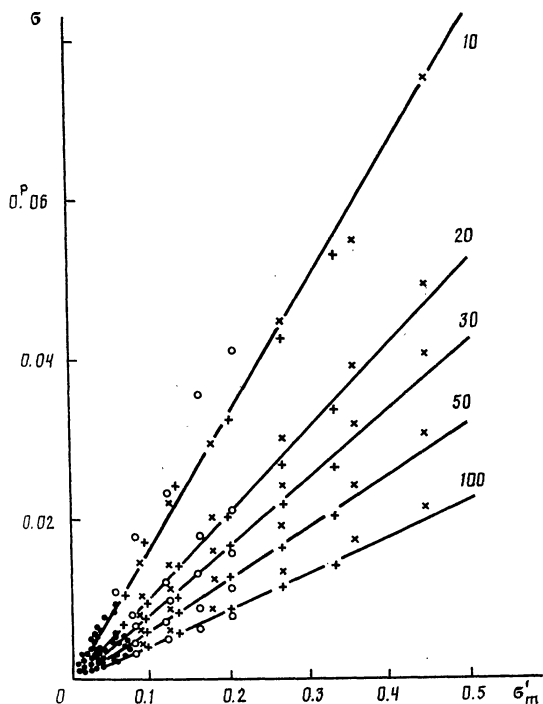


FIG. 1. Error in determining the time of maximum light of Cepheids σ (in fractions of the period) vs the mean-square error in the observations σ_m' (in fractions of the amplitude) for different numbers of observations n . The straight lines for given n are drawn in accordance with equation (3). The data pertaining to different types of light curves are designated by different symbols — crosses for U Aql, circles for SZ Aql, and diagonal crosses for FN Aql. Near the beginning of the coordinates, due to lack of space, all the data are represented by points.

specified amount $\Delta\varphi$, we randomly selected n points. Normally distributed random noise with rms error σ_n was added to the magnitude at each point. The values 10, 20, 30, 50, and 100 were used for n , and $0^m.01$, $0^m.02$, $0^m.03$, $0^m.04$, $0^m.05$, $0^m.07$, $0^m.10$, $0^m.15$, $0^m.20$, and $0^m.25$ for σ_m . This set of n and σ_m values allows us to model any light curves encountered

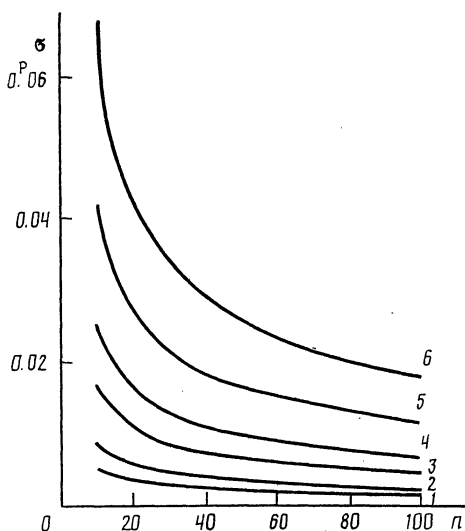


FIG. 2. σ vs n for fixed σ_m' , constructed from Eq. (3). The numbers 1 through 6 designate curves for which σ_m' equals 0.03, 0.05, 0.10, 0.15, 0.25, and 0.40, respectively.

TABLE II

Coefficients in (2)	ϵ	Coefficients in (2)	ϵ
a	0.00176	a, b	0.00141
b	0.00400	b, c	0.00213
c	0.00871	a, c	0.00139
		a, b, c	0.00139

in practice, from high-quality photoelectric ones to poor-quality photographic ones.

For each possible n and σ_m combination we constructed a sample of 100 independent curves, which we then processed by the Hertzprung method. For each sample, Table I gives the calculated values of $\Delta = \bar{\varphi}_{\max} - \Delta\varphi$ (i.e., the differences between the arithmetic mean of the calculated phases at maximum light $\bar{\varphi}_{\max}$ and the specified shift $\Delta\varphi$) and σ , the arithmetic mean of the errors in determining φ_{\max} . Hereafter, σ is expressed in fractions of the period. As is clear from Table I, Δ always equals zero to within the errors, which indicates correct operation of the program.

The data from Table I can be used to find a relationship between the error in determining the time of maximum light σ , the rms error in the processed observations σ_m , and the number of observations n . To elucidate this relationship, we plot σ versus σ_m in Fig. 1 for different values of n . It turns out that if $\sigma_m' = \sigma_m/A$ is used to represent the observational error in Fig. 1 (i.e., the error is expressed as a fraction of the amplitude of brightness variation A), then the dependence of σ on the shape of the light curve becomes weak, and the symbols in Fig. 1 lie along straight lines corresponding to the specified n values. If σ is plotted as a function of n , then the points lie along curves with shapes resembling an inverse proportion, each of which corresponds to a given σ_m' (see Fig. 2). Therefore, we seek σ as a function of n and σ_m' in the form

$$\sigma = \sigma_m' \left(\frac{a}{\sqrt{n}} + \frac{b}{n} + \frac{c}{n^2} \right), \quad (2)$$

where the unknown coefficients a , b , and c are determined by the least squares method.

Table II contains the values of the rms deviation ϵ , characterizing the goodness of fit of Eq. (2) to the data of Table I for all possible combinations of terms in formula (2). The coefficients corresponding to the last row of Table II are $a = 0.454 \pm 0.032$, $b = 0.005 \pm 0.233$, and $c = 2.54 \pm 1.28$, where the b term turns out to be negligible. Removing it from (2) does not change ϵ , and the coefficients become $a = 0.453 \pm 0.006$, and $c = 2.51 \pm 0.27$. Thus, (2) assumes the form

$$\sigma = \sigma_m' \left(\frac{0.453}{\sqrt{n}} + \frac{2.51}{n^2} \right). \quad (3)$$

Equation (3) is used to draw the straight lines in Fig. 1 and to construct Fig. 2, in which σ is plotted vs n for fixed σ_m' .

Some practical recommendations. We have studied Cepheid period variations using observations in different parts of the spectrum, mainly in the V and B bands of the Johnson system, and in the visual and photographic systems approximating these bands. In these studies, we have consistently ignored the fact that the times of maximum light at long wave-

lengths lag those measured at short wavelengths. Our experiment (Berdnikov, 1990) shows that the effect of this lag is entirely measurable, and thus all the times can be reduced to one spectral band. For example, if the majority of observations are in V , then the natural band to consider is V , and the corresponding correction ΔT_B to the times obtained in processing B observations can be determined if these observations are processed relative to the standard curve constructed in V . The similarity of the curves in B and V allows this to be done accurately, and the correction ΔT_V obtained by processing the V observations relative to the standard curve in B can serve as a control. ΔT_B and ΔT_V should be equal in magnitude and opposite in sign.

We assumed that all of the standard curves are in phase. However, it is difficult to place the maxima of all the standard curves precisely at phase "zero." Therefore the phase shifts of the standard curves relative to each other should be determined, and these shifts should be taken into account when calculating the times of maximum light. This approach introduces a degree of uncertainty into the times obtained, but since this uncertainty is systematic, it turns out to have no effect on the $O - C$ curves.

Equation (3), like Figs. 1 and 2, can be used to determine the suitability of the observations to study the stability of

periods to a given level of precision. For example, to search for period changes at the 1% level, the useful curves are those containing about a hundred photoelectric observations. Therefore, long time series containing a large number of photoelectric observations can be divided into "seasons," which increases the number of experimental points, and thereby enhances the temporal resolution of the $O - C$ diagram. An order of magnitude more photographic and visual observations are required to attain this same precision, which, considering the earlier discussion, can smear out the effects of rapid period variability.

Berdnikov, L. N. (1983). *Astron. Tsirk.*, No. 1274, 5.

Berdnikov, L. N. (1990). *Astron. Zh.* 67, 798 [*Sov. Astron.* 34, 400 (1990)].

Tsessevich, V. P. (1971). *Variable Star Research Methods* [in Russian], V. B. Nikonov (ed.), Nauka, Moscow, p. 49.

Translated by J. A. Guzik

Chaotic motion of nearly parabolic comets perturbed by the planets

V. V. Emel'yanenko

Chelyabinsk State Technical University

(Submitted December 10, 1991)

Pis'ma Astron. Zh. 18, 528–536 (June 1992)

We have obtained an analytic expression for the diffusion coefficient of arbitrary, almost parabolic orbits in the restricted circular three-body problem. We give formulas and recursion relations suitable for calculation. The diffusion coefficient is computed for different perihelion distances and orbital inclinations, taking into account perturbations from all of the major planets.

Introduction. The investigation of the long-term evolution of nearly parabolic orbits subject to planetary perturbations is a central problem in the study of the origins of comets, and in the interaction of observed long-period and short-period comets. The principal characteristic of the perturbing action of the planets is the variability of the reciprocal of the semimajor axis of the comet orbit per unit time (the diffusion coefficient). Determination of the diffusion coefficient is the subject of many papers [see, e.g., Everhart (1968); Yabushita (1972); Fernandez (1981); and Danken et al. (1987)]. Numerical modeling of the problem requires integration of the equations of motion of a very large number of comets over long time intervals, and therefore results have been obtained only for certain special cases.

Petrosk (1986), Vecheslavov and Chirikov (1986), and Emel'yanko (1990a) used various approaches to construct an algebraic representation describing the dynamics of objects with orbital periods about the sun exceeding the periods of the perturbing planets. Using this representation, one can find the dependence of the diffusion coefficient on the orbital elements

in the exterior version of the restricted circular three-body problem (Emel'yanenko, 1990b).

In this paper we consider the general case of arbitrary, nearly parabolic orbits. Using analytic expansion of the perturbing functions as proposed by Emel'yanenko (1991), we estimate the diffusion rate of cometary orbits perturbed by the major planets.

Resonant part of the perturbing function in the restricted circular three-body problem. We consider motion of a comet in a nearly parabolic orbit in the gravity field due to the sun and a planet of mass p_m . We use the barycentric form of the equations of motion and the astronomical system of units. According to Emel'yanenko (1991), the perturbing function R of the restricted circular three-body problem can be represented in the form

$$R = R_1 + R_2,$$

$$R_1 = \mu^2 m_p \left\{ \frac{1}{r+r_p} - \frac{1}{r} + \sum_{\alpha=1}^{\infty} \sum_{k=0}^{\alpha} \sum_{s=0}^k \sum_{s'}^{s'} \frac{(\alpha+1)_{\alpha} (\alpha-k+1)_k (2k+1)}{(1)_{\alpha+k+1}} \times \right.$$